Differential Capacity for High-Affinity Manganese Uptake Contributes to Differences between Barley Genotypes in Tolerance to Low Manganese Availability[1]

Pai Pedas, Christopher A. Hebbern, Jan K. Schjoerring, Peter E. Holm, and Søren Husted*

Plant and Soil Science Laboratory, Department of Agricultural Sciences (P.P., C.A.H., J.K.S., S.H.), and Department of Natural Sciences (P.E.H.), Royal Veterinary and Agricultural University, DK–1871 Frederiksberg C, Copenhagen, Denmark

There is considerable variability among barley (*Hordeum vulgare*) genotypes in their ability to grow in soils containing a low level of plant available manganese (Mn). The physiological basis for the tolerance to low Mn availability is unknown. In this work, Mn^{2+} influx and compartmentation in roots of the Mn-efficient genotype Vanessa and the Mn-inefficient genotype Antonia were investigated. Two separate Mn transport systems, mediating high-affinity Mn^{2+} influx at concentrations up to 130 nM and low-affinity Mn^{2+} influx at higher concentrations, were identified in both genotypes. The two genotypes differed only in high-affinity kinetics with the Mn-efficient genotype Vanessa having almost 4 times higher V_{max} than the inefficient Antonia, but similar K_m values. Online inductively coupled plasma-mass spectrometry measurements verified that the observed differences in high-affinity influx resulted in a higher Mn net uptake of Vanessa compared to Antonia. Further evidence for the importance of the differences in high-affinity uptake kinetics for Mn acquisition was obtained in a hydroponic system with mixed cultivation of the two genotypes at a continuously low Mn concentration (10–50 nM) similar to that occurring in soil solution. Under these conditions, Vanessa had a competitive advantage and contained 55% to 75% more Mn in the shoots than did Antonia. Subcellular compartmentation analysis of roots based on $^{54}Mn^{2+}$ efflux established that up to 93% and 83% of all Mn was present in the vacuole in Vanessa and Antonia, respectively. It is concluded that differential capacity for high-affinity Mn influx contributes to differences between barley genotypes in Mn efficiency.

Manganese (Mn) is an essential element for plants and is involved in many cellular processes, including activation of enzymes in lignin biosynthesis and amino acid biosynthesis (Marschner, 1995). In addition, Mn is bound in the O_2 evolving four-atom Mn cluster located on the luminal surface of the D1 protein in PSII and in the scavenging of superoxides by Mn superoxide dismutase in the mitochondria (Britt, 1996; Clemens et al., 2002). Mn-deficient plants have reduced content of fructans and structural carbohydrates causing slack and soft leaves (Pearson and Rengel, 1997). Accordingly, Mn-deficient plants are susceptible to low temperatures and pathogen infections, the latter including the frequently observed take-all (*Gaeumannomyces graminis*) fungal disease (Brennan, 1992; Rengel et al., 1994).

Mn deficiency is a serious plant nutritional disorder in many areas of the world, often associated with increasing soil pH, which favors oxidation to plant unavailable MnO_2. There is considerable variability among plant species and among genotypes of the same species in their ability to grow in soil with low Mn availability, a phenomenon referred to as differential Mn efficiency (Pallotta et al., 2000; Ascher-Ellis et al., 2001; Hebbern et al., 2005). In a screening of 32 barley (*Hordeum vulgare*) genotypes in Australia, it was shown that the most Mn-efficient barley genotypes were largely unaffected by low plant availability of Mn, whereas the most inefficient ones were not able to complete a full life cycle (Graham et al., 1983). Recently, large differences were also observed among European winter barley genotypes (Hebbern et al., 2005). Despite the fact that differential Mn efficiency in plants has been known for more than two decades (Graham, 1988; Ascher-Ellis et al., 2001), the physiological mechanisms are not known. The following factors have been proposed to contribute to differential Mn efficiency: Mn content in the germinating seed; exudation of Mn-chelating and/or Mn-reducing compounds from roots; Mn uptake kinetics; Mn requirement of Mn-dependent key enzymes; subcellular compartmentation of Mn; and, finally, the population of Mn oxidizing and reducing microorganisms in the rhizosphere (Graham, 1988; Graham and Rengel, 1993; Huang et al., 1994). The genetic background for these mechanisms is not known, but it has been possible via RFLP mapping to link a locus in barley to Mn efficiency (Pallotta et al., 2000).

Recently, saturable high- and low-affinity zinc (Zn) transport systems operating in the micromolar and

* Corresponding author; e-mail shu@kvl.dk; fax 4535283460.

The author responsible for distribution of materials integral to the findings presented in this article in accordance with the policy described in the Instructions for Authors (www.plantphysiol.org) is: Søren Husted (shu@kvl.dk).

Article, publication date, and citation information can be found at www.plantphysiol.org/cgi/doi/10.1104/pp.105.067561.

nanomolar range, respectively, were identified in bread wheat (*Triticum aestivum*; Hacisalihoglu and Hart, 2001). The high-affinity transport system (HATS) operates in the range of the low available Zn concentrations found in most soils and is therefore likely to be the predominant Zn^{2+} uptake system (Hacisalihoglu et al., 2001). Similar information does not exist for Mn influx, where the only kinetic data originate from old studies with excised barley or maize (*Zea mays*) roots at fairly high and nonphysiological Mn concentrations in incomplete nutrient solutions (Maas et al., 1968; Landi and Fagioli, 1983).

The objective of this study was to examine the kinetics of Mn^{2+} influx in intact roots of two winter barley genotypes differing in Mn efficiency. Two concentration intervals were examined; 0.1 to 7.8 nM Mn^{2+}, representing soils with low Mn availability, and 10 nM to 655 μM for higher to potentially toxic Mn levels. The radiotracer ($^{54}Mn^{2+}$) influx experiments were complemented by studies of net Mn uptake using a novel online nutrient depletion technique with continuous measurement of Mn and other trace elements by inductively coupled plasma-mass spectrometry (ICP-MS). The competitive abilities of the two genotypes for low Mn concentrations were investigated in a mixed cultivation system with a constant low Mn concentration (10–50 nM) similar to that occurring in soil solution. Finally, the subcellular Mn compartmentation in roots was examined using long-term $^{54}Mn^{2+}$ loading and $^{54}Mn^{2+}$ efflux analysis in order to assess possible differences in internal Mn use efficiency.

RESULTS

Selection of Barley Genotypes Differing in Mn Efficiency

A field-based screening using eight different winter barley genotypes commonly grown in Denmark was established in order to identify genotypes with marked differences in Mn efficiency. Two genotypes differed considerably in growth performance and in severity of Mn deficiency symptoms (Fig. 1). The leaves of the genotype Antonia were highly affected by characteristic Mn deficiency symptoms, such as intervenous necrotic spots developed on a chlorotic background and a limp appearance. Most plants were not able to complete a full life cycle unless treated with Mn foliar sprays. In contrast, the genotype Vanessa was not affected by Mn deficiency as indicated by the absence of leaf symptoms and a growth response to Mn foliar sprays, respectively. Accordingly, Antonia was designated as Mn inefficient and Vanessa as Mn efficient.

Online Measurement of Mn Net Uptake

By the use of ICP-MS, root net uptake of several essential nutrients down to subnanomolar concentrations was analyzed online with very high accuracy (>95%). The Mn-efficient genotype Vanessa had a sig-
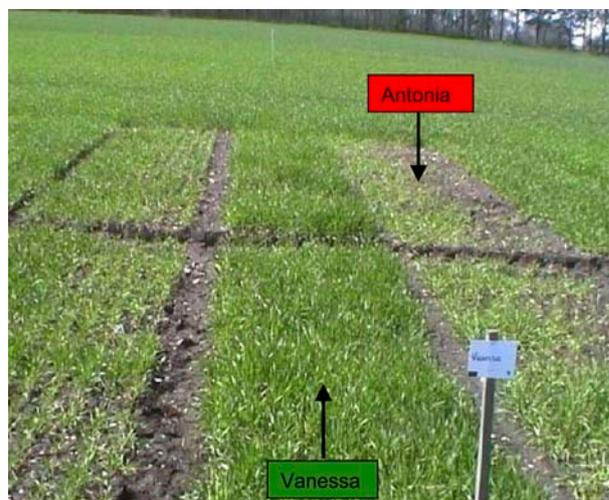

Figure 1. Two winter barley genotypes, Vanessa (Mn efficient) and Antonia (Mn inefficient), grown in a Danish soil with a low plant availability of Mn. The left-hand side of each plot was compacted with a roller immediately after sowing, whereas the right-hand side was left untreated. The Mn concentration in the shoots were in the non-compacted side 24.7 $\pm$ 1.0 and 12.7 $\pm$ 4.7 μg Mn g^{-1} DW for Vanessa and Antonia, respectively, and 26.3 $\pm$ 1.6 and 18.0 $\pm$ 3.5 μg Mn g^{-1} DW for the corresponding compacted side. The photo was taken in early spring.

nificantly higher Mn net uptake compared to the Mn-inefficient genotype Antonia (Fig. 2). Over a 3-h period, Vanessa reduced the Mn concentration from 30 to 10 nM, whereas Antonia only managed to reduce the concentration to 20 nM. After 6 h, the Mn concentration had declined to 5 and 15 nM for Vanessa and Antonia, respectively. A pulse of 30 nM Mn added after 6.5 h was very quickly depleted to below 5 nM by Vanessa, but not by Antonia (Fig. 2). Of all the micronutrients monitored, Mn was by far the most dynamic in the 5 to 30 nM concentration range and was the only one for which a genotypic difference was observed (data not shown). The observed difference in Mn uptake between the genotypes differing in Mn efficiency was confirmed in six independent experiments ($n = 6$) covering Mn concentrations up to 1 μM.

Kinetics of Root $^{54}Mn^{2+}$ Influx

The differential Mn net uptake capacity of the two genotypes was further explored by kinetic studies of unidirectional influx over a 10-min period. Two different concentration ranges were used, namely, 0.1 to 7.8 nM for the HATS and 10 nM to 655 μM for the low-affinity transport system (LATS).

The Mn influx differed very much between the two genotypes in the high-affinity concentration range (Fig. 3). Following Hacisalihoglu et al. (2001) and Hart et al. (1998), the kinetics of root $^{54}Mn^{2+}$ was graphically resolved into saturable and linear components, respectively (Figs. 3, B and C, and 4, B and C), where the latter describes Mn absorbed to cell walls. Vanessa
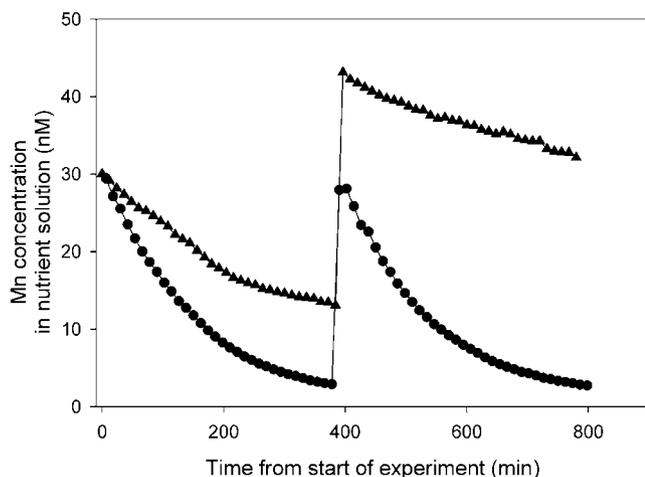
Figure 2. A representative plot of Mn net uptake by the Mn-efficient barley genotype Vanessa (circles) and the Mn-inefficient barley genotype Antonia (triangles) as measured by online ICP-MS. The plants were pregrown in 25 d as described in "Materials and Methods." After 400 min from the start of experiments, a single-pulse addition of Mn was given. The experiments were repeated three times with similar results. Neither root nor shoot weights differed ($P > 0.05$): 0.71 and 0.70 g DW for roots of Vanessa and Antonia, respectively, and 0.75 and 0.75 g DW for the corresponding shoots.

had a maximum uptake capacity (V_{max}) of 5.8 nmol Mn g^{-1} dry weight (DW) h^{-1}, which was almost 4 times higher than that of Antonia, while there was no difference in the K_m value, which ranged from 2.7 to 5.4 nM (Table I). Saturation (>95%) of HATS was estimated to occur at approximately 130 nM Mn^{2+}.

In the low-affinity concentration range, i.e. at high external Mn concentrations, influx values did not differ between the genotypes (Fig. 4). Consequently, there were no significant differences in LATS kinetics, showing a V_{max} of approximately 9 μmol Mn g^{-1} DW h^{-1} and K_m of approximately 100 μM (Table II). It is noteworthy that the plants showed a tremendous capacity to absorb Mn at high concentrations. The uptake rates facilitated by LATS would inevitably lead to Mn toxicity if ample Mn was available for just a few hours and if no system to mediate efflux was present.

Mn Uptake at Continuous Low Nanomolar Mn Concentration

When the two genotypes were grown in different units of the same chemostatic system, with recirculating nutrient solution at low Mn concentrations (10–50 nM), the Mn-efficient genotype Vanessa accumulated approximately 55% and 75% more Mn in the shoot after 25 and 32 d, respectively, than did the inefficient genotype Antonia (Fig. 5). The root and shoot biomass production of the two genotypes did not differ significantly ($P > 0.05$; see Table III). The shoot dry-matter Mn concentration was at both harvest occasions approximately 60% higher in Vanessa than Antonia, while the two genotypes behaved op-

positely in terms of root dry-matter Mn concentration (Table III).

Root Compartmental Analysis

The subcellular compartmentation of Mn in roots of Mn-sufficient barley genotypes with contrasting Mn efficiency was studied by analyzing ^{54}Mn radiotracer efflux from roots over a 5-h period following preloading with ^{54}Mn for 24 h. The remaining ^{54}Mn in the root tissue was calculated and plotted against time. The efflux curves were dissected into three distinct linear components, corresponding to the size of the vacuolar (slow phase; Fig 6A), cytoplasmic (intermediate
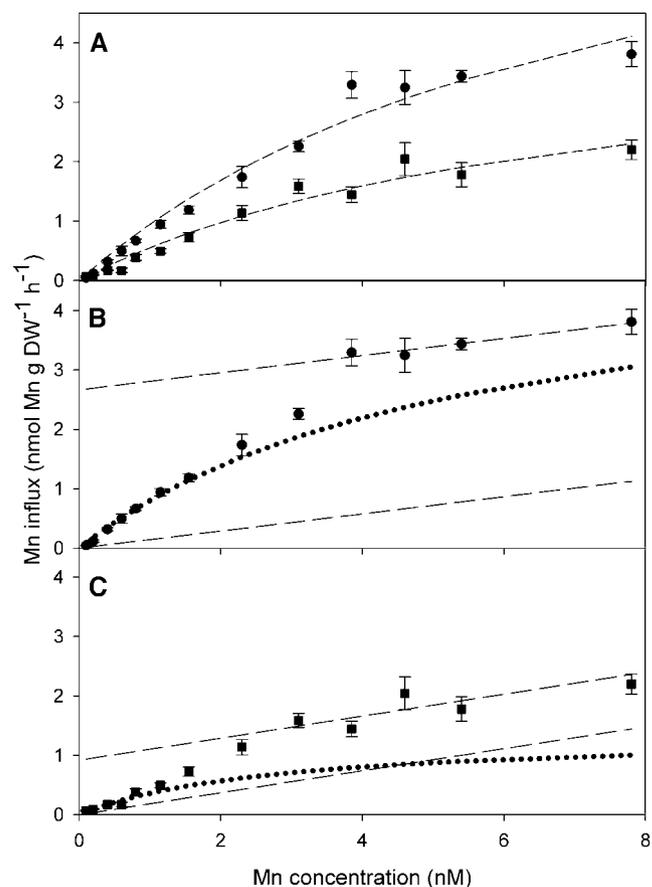

Figure 3. A, Concentration-dependent kinetics for high-affinity ^{54}Mn^{2+} influx in 10-d-old plants of the Mn-efficient barley genotype Vanessa (circle) and the Mn-inefficient barley genotype Antonia (square) at low Mn concentrations (0.1–7.8 nM). The data were fitted to the Michaelis-Menten equation by nonlinear regression (dashed line). B and C, Calculated saturable uptake kinetics from Vanessa and Antonia, respectively, obtained as follows: The linear (dashed line) and saturable (dotted curve) components were derived from the experimental data (circles or squares) by first computing the linear component of the regression line (dashed) plotted through high-concentration points and subsequently subtracting this contribution from the experimental data in order to obtain the saturable influx component by nonlinear Michaelis-Menten regression analysis. The kinetics was estimated using the Michaelis-Menten equation (dotted curves). Error bars represent means ($n = 4$) ± SE.

Pedas et al.

Table I. *Kinetic parameters for high-affinity root Mn^{2+} influx in 10-d-old plants of the barley genotypes Antonia (Mn inefficient) and Vanessa (Mn efficient)*

Values for V_{max} and the apparent K_m were obtained by fitting calculated data of root Mn influx at external Mn^{2+} concentrations ranging from 0.1–7.8 nM to the Michaelis-Menten equation using nonlinear regression analysis (Fig. 3). Root DWs ($P > 0.05$) were 28.3 and 26.7 mg for Vanessa and Antonia, respectively, and the corresponding shoot DWs were 133 and 125 mg, both being nonsignificant. For both genotypes, the Mn concentration in the roots was approximately 70 μg g^{-1} DW. Values with the same superscript letter were not significantly different between genotypes. The results are means $\pm$ 95% confidence limits of four independent regressions ($n = 4$).

HATS	V_{max}	K_m	Regression Coefficient
	nmol Mn g^{-1} DW h^{-1}	nM	R^2
Antonia	1.4 ± 0.4^b	2.7 ± 1.6^a	0.998
Vanessa	5.4 ± 1.0^a	5.4 ± 1.8^a	0.980

component; Fig 6B), and cell-wall-bound Mn pool (fastest component; Fig 6C). For both genotypes, by far the most Mn was stored in the vacuole (83%–93%; Table IV). However, cytoplasmic Mn constituted 13% of the total Mn in the inefficient genotype Antonia, a proportion about 3-fold higher than that in the efficient genotype Vanessa. Also, cell-wall-bound Mn was higher in Antonia, constituting about 4% of total Mn compared to only 1.7% in Vanessa (Table IV). The half-life for Mn efflux in the roots was 2.3 and 1.6 times higher from the vacuole and cytoplasm, respectively, for Vanessa compared with Antonia. No significant difference between the genotypes in half-life Mn efflux from the cell wall was observed.

DISCUSSION

Kinetics for Mn Influx

ICP-MS online measurements revealed that the Mn-efficient genotype Vanessa had a faster net uptake of Mn than the Mn-inefficient genotype Antonia at external Mn concentrations below 50 nM (Fig. 2). This difference reflected the fact that Vanessa had almost 4 times higher maximum uptake capacity (V_{max}) per unit root DW compared to Antonia, while there was no difference in the K_m value, which ranged from 2.7 to 5.4 nM (Table I). The identification of a HATS for Mn, operating in the low nanomolar range, is new and highly relevant for Mn acquisition by plants because the Mn concentration in bulk soil solution normally is in the low micromolar range (Linehan et al., 1989). Diffusion limitation may further reduce the Mn^{2+} concentration in the rhizosphere to a level considerably below that in the bulk soil solution, thereby increasing the importance of effective uptake in the low nanomolar range. Under such conditions, a high ability of roots to capture Mn^{2+} in competition with Mn-oxidizing rhizosphere microorganisms also becomes very favorable.

The observation of substantial genotypic differences in Mn uptake kinetics apparently contradicts that of Huang et al. (1994), who were not able to find any differences between genotypes when grown in solution culture, whereas marked differences could be observed when grown in soil with low Mn availability. However, it is likely that Huang et al. (1994) might have exposed plants to far higher and more fluctuating Mn concentrations than were actually intended (4–400 nM, maintained by addition of EDTA). Maintaining low nanomolar concentrations is a real challenge and major discrepancies are likely to occur between theoretical and actual low nanomolar concentrations, unless chemicals are purified by chelation resin to remove traces of Mn. Furthermore, in the study by Huang et al. (1994), the cultivation solution was only renewed every fourth day, which may have led to nutrient depletion and secondary responses masking differential Mn efficiency. In our work, genotypic differences were repeatedly and reproducibly obtained within a few weeks when plants were grown at
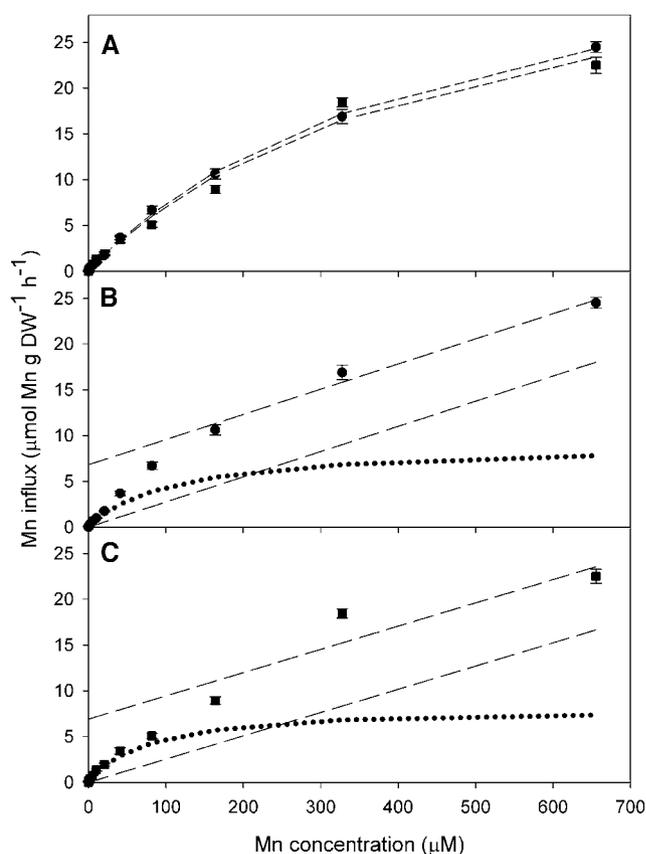

Figure 4. A, Concentration-dependent kinetics for low-affinity $^{54}Mn^{2+}$ influx in 10-d-old plants of the Mn-efficient barley genotype Vanessa (circle) and the Mn-inefficient barley genotype Antonia (square) at Mn concentrations (10 nM–655 μM). The data were fitted to the Michaelis-Menten equation by nonlinear regression (dashed line). B and C, Calculated saturable uptake kinetics from Vanessa and Antonia, respectively, obtained as described in Figure 3. The kinetics was estimated using the Michaelis-Menten equation (dotted lines). Error bars represent means ($n = 4$) $\pm$ SE.

1414

Table II. *Kinetic parameters for low-affinity root Mn²⁺ influx in 10-d-old plants of the barley genotypes Antonia (Mn inefficient) and Vanessa (Mn efficient)*

Values for V_{max} and the apparent K_m were obtained by fitting calculated data of root Mn influx at external Mn^{2+} concentrations ranging from 10 nM to 655 μM to the Michaelis-Menten equation using nonlinear regression analysis (Fig. 4). Plant characteristics are as in Table I. Values with the same superscript letter were not significantly different between genotypes. The results are presented as average $\pm$ 95% confidence limits of four independent regressions ($n = 4$).

LATS	V_{max}	K_m	Regression Coefficient
	$\mu mol\ Mn\ g^{-1}\ DW\ h^{-1}$	μM	R^2
Antonia	9.1 ± 1.4^a	109 ± 50^a	0.980
Vanessa	8.5 ± 0.5^a	79 ± 15^a	0.990

a continuously low nanomolar concentration, maintained by daily addition of Mn based on results from ICP-MS measurement of the actual Mn concentration. By this strategy, it was possible to keep plants on a low-Mn diet where no Mn deficiency symptoms (such as chlorosis) were allowed to develop in order to avoid secondary symptoms and responses that might influence Mn uptake kinetics. However, it is important to note that the genotypes used in this experiment and in studies performed by Huang et al. (1994) are genetically different. Thus, different mechanisms of

Mn efficiency might be involved in the plants used for these two studies.

In addition to the HATS system, a LATS system was identified with a K_m of 80 to 110 μM (Table II), approximately one-fourth of that observed for excised maize roots by Landi and Fagioli (1983). A similar K_m value of 400 μM was reported for excised barley roots by Maas et al. (1968). In all cases, the uptake rates facilitated by LATS would, within a few minutes, lead to Mn toxicity (Mn tissue concentration >150 μg Mn g^{-1} DW) if no system to mediate Mn efflux was present. There is currently no documentation of a Mn efflux system in plants, even though several calcium pumps have been shown to have the ability to co-transport Mn (Dürr et al., 1998; Baelen et al., 2001; Wu et al., 2002).

The importance of the observed difference in V_{max} for Mn uptake at low nanomolar concentrations (Table I) was further demonstrated in a mixed cultivation system where the two genotypes were grown under conditions where Mn concentrations were maintained in the range from 10 to 50 nM. Vanessa, i.e. the efficient genotype with the highest V_{max}, had under these conditions a competitive advantage over Antonia, which was manifested in 55% and 75% higher Mn acquisition in shoots after 25 and 32 d, respectively (Fig. 5). Independent experiments, where the two barley geno-
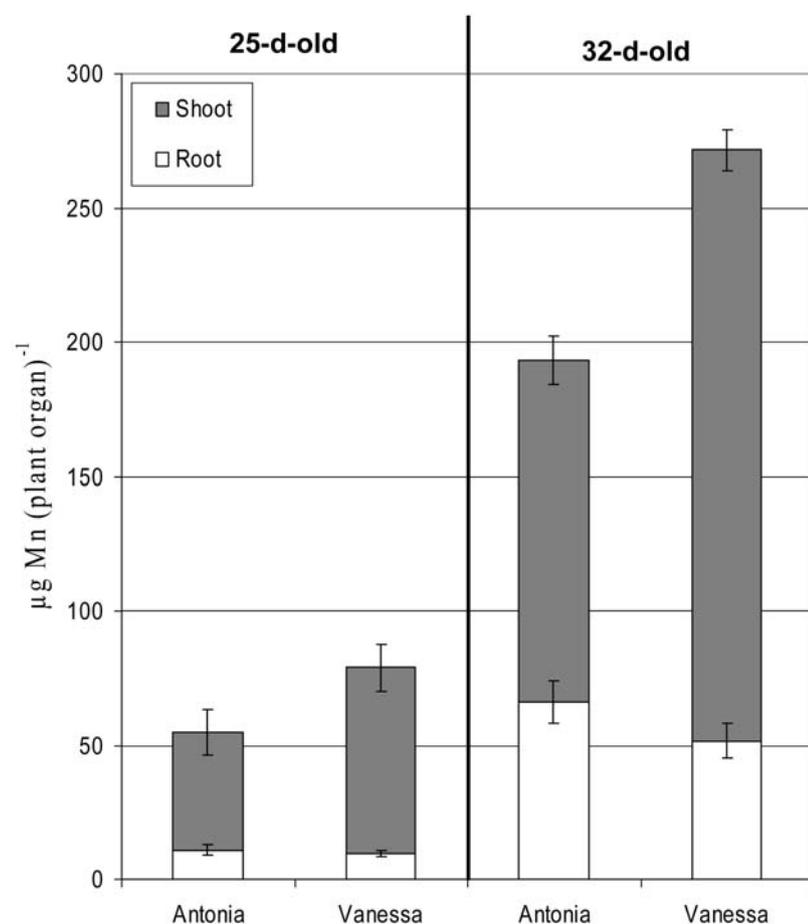

Figure 5. Accumulated Mn content in roots (white area) and shoots (gray area) of the Mn-inefficient barley genotype Antonia and the Mn-efficient barley genotype Vanessa grown at continuous low (10–50 nM) Mn concentrations for 25 and 32 d, respectively. Error bars represent means ($n = 4$) $\pm$ SE.

Table III. *Shoot and root dry-matter weights and Mn concentrations for the Mn-efficient barley genotype Vanessa and the Mn-inefficient barley genotype Antonia grown in a hydroponic system with mixed cultivation of the two genotypes at a continuously low Mn concentration (10–50 nM)*

Values are means ± SE (n = 4).

	Days	Root	Shoot	Root	Shoot
		Biomass		Mn Concentration	
		g DW		μg g⁻¹ DW	
Antonia	25	0.35 ± 0.01	1.49 ± 0.08	31.8 ± 6.7	29.3 ± 5.2
	32	0.79 ± 0.10	3.50 ± 0.43	83.7 ± 5.6	37.0 ± 3.9
Vanessa	25	0.33 ± 0.04	1.47 ± 0.17	29.6 ± 1.2	46.6 ± 1.5
	32	0.96 ± 0.09	3.76 ± 0.45	54.5 ± 5.0	59.7 ± 4.0

types were grown with 500 and 1,000 nM Mn concentrations with renewal three times a week, did not show a difference in total Mn content (data not shown). The differential capacity for Mn uptake was thus lost during growth at Mn concentrations in the LATS range where the two genotypes did not differ from each other with respect to uptake kinetic parameters (Fig. 4; Table II).

Correction for binding of ^{54}Mn to cell walls during the influx experiments was carried out following the procedure used for Zn^{2+} adsorption by Hacisalihoglu et al. (2001) and Hart et al. (1998). This procedure is based on subtraction of the linearly increasing part of the influx curve, which may be due to adsorption, from the total uptake curve, reflecting true uptake into the cells, the saturable component (Figs. 3, B and C, and 4, B and C). For Mn^{2+}, the correction only had a minor influence on the relative differences between the genotypes in uptake kinetic parameters. Significant adsorption of Mn^{2+} would actually not be expected, as Mn according to the Irving-Williams series forms weak complexes compared with Zn (Stumm and Morgan, 1981). A good agreement between genotypic differences in influx kinetics (Table I) and net uptake rates
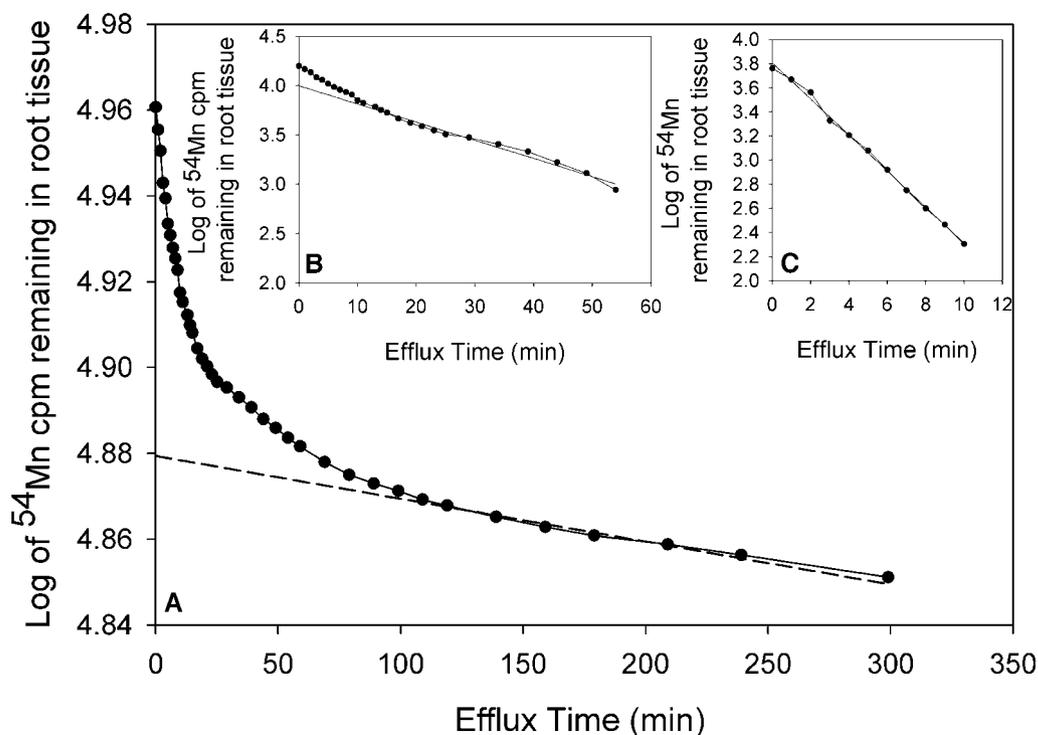

Figure 6. Time course of Mn efflux from 13-d-old barley roots (genotype Vanessa) preloaded with ^{54}Mn. The remaining ^{54}Mn in the root tissue was calculated and plotted against time. The regression lines were drawn through the linear part of the curve and extrapolated to a given value at time zero. The extrapolation to time zero in A represents the size of the vacuolar Mn pool. Subtraction of the linear component from the data points in A produced the curve in B, which linear part represents the cytoplasmic Mn pool. A similar procedure was used to obtain the value in C representing the cell-wall-bound Mn pool. The mean values of five independent regression estimates similar to the one outlined above are listed in Table I. R^2 values for A and B were always >0.99 and for C >0.93.

Table IV. *Subcellular Mn distribution and half-life ($t_{1/2}$) for Mn efflux in roots of barley genotypes differing in Mn efficiency*

Thirteen-day-old plants were pregrown as described in "Materials and Methods." The results are presented as average $\pm$ SE ($n = 5$). Values with the same superscript letter were not significantly different between genotypes ($P > 0.05$).

Genotype	Vacuole		Cytoplasm		Cell Wall	
	Mn	$t_{1/2}$	Mn	$t_{1/2}$	Mn	$t_{1/2}$
	%	*h*	*%*	*min*	*%*	*min*
Antonia	83.4 ± 1.0^b	54.4 ± 1.4^b	12.9 ± 1.2^a	17.5 ± 1.9^b	4.1 ± 1.1^a	1.4 ± 0.4^b
Vanessa	92.8 ± 0.6^a	123.0 ± 20.1^a	4.8 ± 0.2^b	27.8 ± 4.2^a	1.7 ± 0.4^b	1.9 ± 0.8^a

(Fig. 2) supports that the kinetic parameters reflect real differences in uptake capacity into the root cells. Thus, influx values at 20 nM, calculated on the basis of the kinetic parameters, were 4.1 and 1.2 nmol g^{-1} DW h^{-1} for Vanessa and Antonia, respectively. The corresponding net uptake rates in the concentration interval from 30 to 10 nM Mn, obtained in the online ICP-MS experiment, were 4.6 and 2.0 nmol g^{-1} DW h^{-1}.

As the affinity (K_m value) of the potential transporter proteins for Mn does not seem to be significantly different between the genotypes, it can be assumed that the actual uptake is carried out with the same transporter proteins, but the expression level of these transporter proteins is higher for the Mn-efficient genotype compared to the Mn-inefficient genotype, but this awaits further investigation. Only a few putative Mn transporters have so far been reported in plants, and in all cases Mn has been shown to be cotransported with several other micronutrients (e.g. Fe and Zn) or nonessential trace elements such as cobalt and lead (for details, see reviews by Guerinot, 2000; Williams et al., 2000; Mäser et al., 2001). Potential transporter families involved in Mn transport in barley include members of the Nramp and ZIP family, which have been documented to have some Mn specificity in rice (*Oryza sativa*), yeast (*Saccharomyces cerevisiae*), and bacteria (Belouchi et al., 1997; Ramesh et al., 2003).

Mn Subcellular Compartmentation

The overall biomass production and root Mn concentration were similar for the two barley genotypes (see "Materials and Methods"), but they differed with respect to the localization of Mn in the root cells. The largest difference was observed for the cell wall and cytoplasm, where the inefficient genotype Antonia had 2- to 3-fold more Mn than Vanessa. However, as by far the major part of root Mn was contained in the vacuoles (83% and 93% for Antonia and Vanessa, respectively), it is unlikely that the cell wall and cytoplasm contribute significantly to the genotypic differences in Mn efficiency (Table IV). This observation is supported by data from Figure 3, where the linear components of the high-affinity uptake curves are nearly identical for the efficient and inefficient genotype. Vanessa seemed to have a stronger capacity to bind Mn in the cell, since the half-life for the vacuolar and cytosolic pools was approximately 2.3 and 1.6 times higher than the corresponding values for Anto-

nia (Table IV). A rapid leakage of Mn ions from the vacuole to the soil solution under Mn limitation might contribute to low Mn efficiency. It would be advantageous to keep a high proportion of the intracellular Mn in less biochemically active compartments such as the vacuole to minimize oxidative stress reactions.

It has been documented that the vacuole is the major Mn storage compartment in leaves from common bean and in roots from maize (Quiquampoix et al., 1993b; González and Lynch, 1999). Whether Mn in the vacuole is present as a free ion or in chelated or precipitated form is currently unclear. Quiquampoix et al. (1993a) suggested that less than 5% of root Mn was present as free Mn^{2+} in the vacuole. In comparison with Fe^{3+}, Cu^{2+}, Zn^{2+}, and Fe^{2+}, Mn^{2+} forms relatively unstable complexes (Stumm and Morgan, 1981). Organic acids, such as citrate, malate, malonate, and oxalate, have been suggested as possible ligands, especially in connection with metal tolerance mechanisms in hyperaccumulating plants (Memon and Yatazawa, 1984; Bidwell et al., 2002), but other metabolites, such as low M_r thiols, amino acids, peptides, and proteins, might also be potential ligands in the acidic vacuolar environment, as observed for several micronutrients (Brune et al., 1994; Persans et al., 1999; Lasat, 2002). Whether a similar correlation between the subcellular compartments is seen in leaf awaits further experiments.

CONCLUSION

Uptake experiments using pH-buffered nutrient solutions revealed the presence of two separate Mn uptake systems in barley, mediating high- and low-affinity Mn^{2+} influx, respectively. Two barley genotypes with differential tolerance toward low Mn availability only differed with respect to high-affinity Mn influx, the Mn-efficient genotype having almost 4 times higher V_{max} than the inefficient, while the K_m values were similar. The identification of a HATS for Mn operating in the low nanomolar range is new and highly relevant for Mn acquisition by plants. Short time scale depletion studies showed that the differences in high-affinity kinetics resulted in a higher (>100%) Mn net uptake rate in the Mn-efficient genotype. When growing together in a mixed hydroponic system with a continuously low Mn concentration (10–50 nM) similar to that occurring in soil solution, the

Mn-efficient genotype had a competitive advantage and contained 55% to 75% more Mn in the shoots than the Mn-inefficient genotype. The results show that differential capacity for high-affinity Mn influx contributes to Mn efficiency differences between barley genotypes.

MATERIALS AND METHODS

$^{54}Mn^{2+}$ Influx Experiments

Seeds of the two different barley (*Hordeum vulgare*) genotypes were germinated at 21°C between two filter papers in the dark. After 5 d, uniform seedlings were selected and transferred to light-impermeable polyethylene boxes (50 L). The seedlings were placed in holes of light-sealed floaters of foam rubber fitted with aeration tubes. There were 36 seedlings per box. The boxes were filled with a chelate-buffered solution prepared in 18.2 M Milli-Q water (Milli-Q Plus; Millipore) containing 200 μM KH_2PO_4, 200 μM K_2SO_4, 300 μM $MgSO_4$-7H_2O, 100 μM NaCl, 300 μM $Mg(NO_3)_2$-6H_2O, 900 μM $Ca(NO_3)_2$-4H_2O, 600 μM KNO_3, 8 μM Na_2MoO_4-2H_2O, 7 μM $ZnCl_2$, 8 μM $CuSO_4$-5H_2O, 2 μM H_2BO_3, 1 μM $NiSO_4$-6H_2O, 50 μM $Fe(NO_3)_3$-9H_2O, and 10 μM EDTA. pH was adjusted with NaOH and HCl to pH 6.0 $\pm$ 0.3. For the first 5 d, the plants were grown with 500 nM $MnCl_2$, then for 5 d with 50 nM $MnCl_2$. The nutrient solution was renewed daily in order to avoid major Mn concentration fluctuations. By the use of Chelex-100 resin (Sigma-Aldrich), the chemicals used for nutrient solution were cleaned for traces of Mn. Plants used for the uptake experiments were grown in a controlled environment growth chamber with a 250 to 280 μmol m^{-2} s^{-1} photon flux density, 75% to 80% humidity, and a 20°C/15°C (16/8 h) day/night temperature regime.

Influx experiments were performed essentially as described by Hacisalihoglu et al. (2001) with few modifications. Experiments were started at times corresponding to the photoperiod of the plants. Intact 10-d-old seedlings were removed from the nutrient solution. The roots were rinsed in 18.2 M Milli-Q-water for 10 min, and placed in 5-L boxes containing pretreatment solution (2 mM MES-Tris, pH 6.0, 0.2 mM $CaSO_4$, 12.5 μM H_3BO_4, 0.5 nM $MnCl_2$) for 30 min. Wells of 70-mL high-density polyethylene glass (Capitol Vial) were filled with 50 mL of uptake solution consisting of 5 mM MES-Tris, pH 6.0, 0.2 mM $CaSO_4$, 12.5 μM H_3BO_4, and varying concentrations of radiolabeled $^{54}Mn^{2+}$ (1,409.44 MBq/mg; Perkin-Elmer Life Science Products) and nonradiolabeled $MnCl_2$ to yield the desired total Mn^{2+} concentration (0.1–7.8 nM Mn^{2+} for the low-concentration range and 10 to 655 μM Mn^{2+} for the high-concentration range). The Mn concentration in the ^{54}Mn-enriched nutrient solutions used to measure Mn^{2+} influx was checked by ICP-MS before initiation of the uptake studies, and the analytical accuracy was found to be better than 85% at concentrations below 5 nM and better than 95% for concentrations higher than 10 nM (data not shown).

The uptake experiments were initiated by gently inserting the roots of intact seedlings into the aerated vials. A sample of the uptake solution was taken as a control and subsequently concentrated by a factor of 10 to a final volume of 5 mL in a vacuum concentrator (Christ Alpha-RVC IR Rotations-Vakuum-Koncentrator). Since preliminary experiments had shown that the accumulated Mn uptake increased linearly with time for at least 15 min after the start of the experiment, 10 min was chosen as the duration for influx measurements. ICP-MS was used to confirm that no significant depletion of Mn took place in the uptake solution during the experimental period.

At the end of the 10-min influx period, plants were gently moved to 200-mL polypropylene wells consisting of ice cold (2°C) desorption solution (5 mM MES-Tris, pH 6.0, 5 mM $CaCl_2$, 100 μM $MnCl_2$). Desorption was performed in the dark at 2°C. After two 7.5-min desorption periods sufficient to remove cell-wall-bound ^{54}Mn remaining in the root apoplast (see compartmental analysis), seedlings were removed from the vials, the roots were blotted with paper towels, freeze dried (Christ Alpha 2-4; Martin Christ GmbH), and weighed. The roots were dissolved in 5 mL concentrated HNO_3. All samples of roots and controls were dissolved in acid and had a total volume of 5 mL, which gave the same distance (volume) from the emitting material to the γ counter. The activity of $^{54}Mn^{2+}$ taken up by the roots and $^{54}Mn^{2+}$ in the control samples was measured using a γ counter (model 14-22; Selektronik). Experiments were performed with four replicates.

Data could be resolved into a linear and saturable component (Figs. 3, B and C, and 4, B and C). The linear component resembles the cell-wall-bound Mn, whereas the saturable component is equivalent to the actual uptake. The actual uptake was then achieved by computing the linear component from the regression line plotted through high-concentration points and subtracting this contribution from the experimental data. The kinetic parameters were derived on the basis of the subtracted data using the Michaelis-Menten equation by means of nonlinear regression analysis via the SAS program (V8; SAS Institute). Residual analysis of the regression estimates confirmed that the Michaelis-Menten equation was able to describe the influx without systematic errors.

Online ICP-MS Measurement of Mn Uptake

An ICP-MS (Agilent 7500c; Agilent Technologies) with a microflow nebulizer was used to analyze the Mn depletion of the nutrient solution as described elsewhere (Husted et al., 2003). A multichannel peristaltic pump continuously recirculated nutrient solution between an autosampler vial (50-mL vial, product no. 02-6100N; CM-LAB) and the cultivation unit with plants. The tube inlet and outlet were vertically displaced in the autosampler tube providing a steady-state volume of approximately 7.5 mL due to a flow rate difference between inlet and outlet. One cultivation unit with one plant and one without (control) were analyzed. During sampling, a mixture of 1.75% HNO_3, 0.2% HF, and 10 mg/L ^{45}Sc was continuously added to the nebulizer (split ratio 1:20) in order to reduce memory effects and to correct for drift and argon plasma instability. Each of the two vials was analyzed every 12 min during the sampling period. In separate experiments, continuous analysis of control nutrient solution without plants documented that no significant interferences caused by, for example, precipitation and adsorption of Mn to surfaces of the experimental system were occurring during the experiments.

The experiments were conducted with seedlings grown in 300-mL vials (Bie and Berntsen) under conditions as described above, except for a few modifications: The seedlings were initially grown with 250 nM $MnCl_2$ in the 300-mL vials for 18 d, then transferred to 500-mL polypropylene vials for 7 d with a reduced micronutrient supply (0.01 μM Na_2MoO_4-2H_2O, 0.01 μM $ZnCl_2$, 0.01 μM $CuSO_4$-5H_2O, 0.01 μM H_2BO_3, 0.01 μM $NiSO_4$-6H_2O, 0.01 μM $Fe(NO_3)_3$-9H_2O, and 100 nM $MnCl_2$). For the first 18 d, the nutrient solution was renewed every second day, and, during the last 7 d, the solution was exchanged every day. Twenty-four hours before the online measurement of nutrient solution was initiated, plants were transferred to a class 10.000 clean room with the ICP-MS facility, and plants were exposed to a 250 to 280 μmol m^{-2} s^{-1} photon flux density and a 20°C (16/8 h) day/night temperature regime. One-half hour before the start of the online uptake experiments, the nutrient solution was renewed with 10 nM $MnCl_2$, whereupon the plants were given a single pulse addition of Mn.

Several preliminary experiments had shown that it was important to equilibrate plants for at least 24 h to the concentration range used in the uptake studies in order to reduce the time needed for equilibrating ion-exchange processes at the root surface. Failure to equilibrate the plant root to the micronutrient concentration in the nutrient solution might lead to a long period (several hours) of continuous liberation of Mn and other micronutrients adsorbed to the root surface. Measuring the solution containing the root fraction alone in ice-cold solution showed that >95% of the depleted Mn could be root recovered during a period of 6 h. After equilibration of the plant roots, no desorption occurred and depletion of the free Mn started instantaneously.

Long-Term Mn Uptake at Continuous Low Nanomolar Mn Concentration

Vanessa and Antonia were grown in a recirculating nutrient solution with the same composition as that used for the $^{54}Mn^{2+}$ influx experiment, with the exception of Mn. Two hundred liters of solution were recirculated through four replicate containers of each genotype, each container holding four plants. The flow rate of the solution through each container was 2 L min^{-1}, corresponding to replacement of the nutrient solution in less than 3 min. Mn chemostasis was controlled by daily measurements by ICP-MS and adjusted, if needed, to obtain a Mn concentration between 10 to 50 nM being relevant for the HATS kinetics. After 25 and 32 d, respectively, plants in four replicate containers were harvested, freeze dried (Christ Alpha 2-4; Martin Christ GmbH), and weighed. The plant material was digested in an open-vessel system using 70-mL high-density polyethylene vials (Capitol Vial) and a graphite-

heating block (Mod-block; CPI International). A slightly modified version of Environmental Protection Agency (EPA) method 3050B was used as described below. Five milliliters of 35% HNO_3 (instra analyzed; Baker) were added to 0.25 g DW of plant material and boiled for approximately 15 min. After cooling, 2.5 mL of 70% HNO_3 were added and the samples were reheated. After 30 min, the samples were cooled and 1.5 mL H_2O_2 (extra pure; Riedel-de Haën) was applied and samples were heated again. When the hydrogen peroxide reaction ceased, an additional 1.0 mL of H_2O_2 was added and samples were boiled for approximately 60 min. During the digestion, the vials were covered with high-density polyethylene glass lids. The samples were cooled overnight and filled up to 50 mL with ultrapure water. For every bath on the mod block, seven blank and seven samples of certified reference material (Apple leaf, standard reference material 1515; National Institute of Standards and Technology) were included to estimate the accuracy and precision of the analysis. All the samples were diluted to the same acid concentration (1.75% HNO_3) and measured on the ICP-MS.

Mn Compartmentation Analysis

The protocol for the subcellular compartmental analysis was modified from Bell et al. (1994). Ten-day-old seedlings of Antonia and Vanessa with similar root and shoot biomass production (63 ± 3 and 243 ± 10 mg for root and shoot, respectively), were grown with full nutrient supplied, as described above, and were starved for Mn for 2 d. The 12-d-old seedlings did not exhibit Mn deficiency symptoms. After starvation, the seedlings were precultured with aeration for 24 h in a solution with 100 nM $MnCl_2$ enriched with 16 μCi $^{54}Mn^{2+}$ per 4 L Milli-Q water and buffered with 5 mM MES-Tris, pH 6.0, 0.2 mM $CaCl_2$, 12.5 μM H_3BO_4. The seedlings were then transferred to the efflux solution (5 mM MES-Tris, pH 6.0, 0.2 mM $CaCl_2$, 12.5 μM H_3BO_4, 100 μM $MnCl_2$, without ^{54}Mn). Subsequently, at various time intervals, the efflux solution was collected and the solution exchanged with fresh efflux solution. After 5 h, plant sections were collected and ^{54}Mn activity in efflux solution samples and plant sections were measured with a γ counter (model 14-22; Selektronik). The samples were concentrated by a factor of 10 to a final volume of 5 mL with a vacuum concentrator (Christ Alpha-RVC IR Rotations-Vakuum-Koncentrator). The ^{54}Mn remaining in the plant tissue was calculated and plotted against time in a semilogarithmic plot. In higher plants, analysis of efflux curves commonly reveals three exponential (first-order) components. The resulting linear component drawn through the last part of the sampling period represents first-order efflux from the slow efflux component in the tissue corresponding to exchange from the vacuolar space and was extrapolated to the y axis. This line was subtracted from the original curve and resultant data were plotted against time corresponding to an efflux curve from the remaining two components (cytoplasm and cell wall). Similarly, subsequent linear components were extracted. Manganese contents (%) were estimated as the y axis intercepts and the half-life ($t_{1/2}$) was the slope of each curve.

ACKNOWLEDGMENT

LITERATURE CITED

Ascher-Ellis JS, Graham RD, Hollamby GJ, Paull J, Davies P, Huang C, Pallotta MA, Howes N, Khabez-Saberi H, Jefferies SP, et al (2001) Micronutrients. *In* MP Reynolds, JI Ortiz-Monasterio, A McNab, eds, Application of Physiology in Wheat Breeding. CIMMYT, Mexico, pp 219–240

Baelen KV, Vanoevelen J, Missiaen L, Raeymaekers L, Wuytack F (2001) The golgi PMR1 P-type ATPase of *Caenorhabditis elegans*. J Biol Chem **276:** 10683–10691

Bell CI, Gram WJ, Clarkson DT (1994) Compartmental analysis of $^{35}SO_4^{2-}$ exchange kinetics in roots and leaves of a tropical legume *Macroptilium atropurpureum* cv. Siratro. J Exp Bot **45:** 879–886

Belouchi A, Kwan T, Gros P (1997) Cloning and characterization of the OsNramp family from Oryza sativa, a new family of membrane proteins possibly implicated in the transport of metal ions. Plant Mol Biol **33:** 1085–1092

Bidwell SD, Woodrow IE, Batianoff GN, Sommer-Knudsen J (2002) Hyperaccumulation of manganese in the rainforest tree *Austromyrtus bidwillii* (Myrtaceae) from Queensland, Australia. Funct Plant Biol **29:** 899–905

Brennan RF (1992) The role of manganese and nitrogen nutrition in the susceptibility of wheat plants to take-all in Western Australia. Fert Res **31:** 35–41

Britt RD (1996) Oxygen evolution. *In* C Yocum, ed, Oxygenic Photosynthesis: The Light Reactions. Kluwer Academic Publishers, Dordrecht, The Netherlands, pp 137–159

Brune A, Urbach W, Dietz KJ (1994) Compartmentation and transport of zinc in barley primary leaves as basic mechanisms involved in zinc tolerance. Plant Cell Environ **17:** 153–162

Clemens KL, Force DA, Britt RD (2002) Acetate binding at the photosystem II oxygen evolving complex: an S(2)-state multiline signal ESEEM study. J Am Chem Soc **124:** 10921–10933

Dürr G, Strayle J, Plemper R, Elbs S, Klee SK, Catty P, Wolf DH, Rudolph HK (1998) The *medial*-golgi ion pump Pmr1 supplies the yeast secretory pathway with Ca^{2+} and Mn^{2+} required for glycosylation, sorting, and endoplasmic reticulum associated protein degradation. Mol Biol Cell **9:** 1149–1162

González A, Lynch JP (1999) Subcellular and tissue Mn compartmentation in bean leaves under Mn toxicity stress. Aust J Plant Physiol **26:** 811–822

Graham R, Davies W, Sparrow D, Ascher J (1983) Tolerance of barley and other cereals to manganese-deficient calcareous soils of South Australia. *In* BC Loughman, ed, Genetic Aspects of Plant Nutrition. Martinus Nijhoff, The Hague, The Netherlands, pp 339–334

Graham RD (1988) Genotypic differences in tolerance to manganese deficiency. *In* RD Graham, RJ Hannam, NC Uren, eds, Manganese in Soils and Plants, Vol 17. Kluwer Academic Publishers, Dordrecht, The Netherlands, pp 261–276

Graham RD, Rengel Z (1993) Genotypic variation in zinc uptake and utilization by plants. *In* AD Robson, ed, Zinc in Soils and Plants. Kluwer Academic Publishers, Dordrecht, The Netherlands, pp 107–114

Guerinot ML (2000) The ZIP family of metal transporters. Biochim Biophys Acta **1465:** 190–198

Hacisalihoglu G, Hart J (2001) Two pieces of the zinc efficiency puzzle: root-Zn influx and Zn-compartmentation in the shoot. *In* WJ Horst, MK Schenk, A Bürkert, N Claassen, H Flessa, WB Frommer, H Goldbach, H-W Olfs, V Römheld, B Sattelmacher, U Schmidhalter, S Schubert, N von Wirén, L Wittenmayer, eds, Plant Nutrition—Food Security and Sustainability of Agro-Systems. Kluwer Academic Publishers, Dordrecht, The Netherlands, pp 192–193

Hacisalihoglu G, Hart JJ, Kochian LV (2001) High- and low-affinity zinc transport systems and their possible role in zinc efficiency in bread wheat. Plant Physiol **125:** 456–463

Hart JJ, Norwell WA, Welch RM, Sullivan LA, Kochian LV (1998) Characterization of zinc uptake, binding and translocation in intact seedlings of bread and durum wheat cultivars. Plant Physiol **118:** 219–226

Hebbern CA, Pedas P, Schjoerring JK, Knudsen L, Husted S (2005) Genotypic differences in manganese efficiency: a field trial with winter barley (*Hordeum vulgare* L.). Plant Soil **272:** 233–244

Huang C, Webb MJ, Graham RD (1994) Manganese efficiency is expressed in barley growing in soil system but not in solution culture. J Plant Nutr **17:** 83–95

Husted S, Holm PE, Hansen HCB, Schjoerring JK (2003) On-line measurement of essential plant nutrient dynamics in the root medium using ICP-MS with an octopole reaction system. *In* 2003 European Winter Conference on Plasma Spectrochemistry, January 12–17, 2003, Garmisch-Partenkirchen, Germany

Landi S, Fagioli F (1983) Efficiency of manganese and copper uptake by excised roots of maize genotypes. J Plant Nutr **6:** 957–970

Lasat MM (2002) Phytoextraction of toxic metals: a review of biological mechanisms. J Environ Qual **31:** 109–120

Linehan D, Sinclair A, Mitchell M (1989) Seasonal changes in Cu, Mn, Zn and Co concentrations in soil solution in the root-zone of barley. J Soil Sci **40:** 103–115

Maas EV, Moore DP, Mason BJ (1968) Manganese absorption by excised barley roots. Plant Physiol **43:** 527–530

Marschner H (1995) Mineral Nutrition of Higher Plants. Academic Press, San Diego, pp 325–329

Mäser P, Thomine S, Schroeder JI, Ward JM, Hirsch K, Sze H, Talke IN, Amtmann A, Maathuis FJ, Sanders D, et al (2001) Phylogenetic relationship within cation transporter families of Arabidopsis. Plant Physiol **126:** 1646–1667

Memon AR, Yatazawa M (1984) Nature of manganese complexes in the manganese accumulator plant *Acanthopanax sciedophylloides.* J Plant Nutr **7:** 961–974

Pallotta MA, Graham RD, Langridge P, Sparrow DHB, Barker SJ (2000) RFLP mapping of manganese efficiency in barley. Theor Appl Genet **101:** 1100–1108

Pearson JN, Rengel Z (1997) Genotypic differences in the production and partitioning of carbohydrates between roots and shoots of wheat grown under zinc or manganese deficiency. Ann Bot (Lond) **80:** 803–808

Persans MW, Patnoe XY, Krämer U, Salt DE (1999) Molecular dissection of the role of histidine in nickel hyperaccumulation in *Thlaspi goesingense* (Hálácsy). Plant Physiol **121:** 1117–1126

Quiquampoix H, Bacic G, Loughman BC, Ratcliffe RG (1993a) Quantitative aspects of the ^{31}P-NMR detection of manganese in plant tissues. J Exp Bot **44:** 1809–1818

Quiquampoix H, Loughman BC, Ratcliffe RG (1993b) A ^{31}P-NMR study of the uptake and compartmentation of manganese by maize roots. J Exp Bot **44:** 1819–1827

Ramesh SA, Shin R, Eide DJ, Schachtman DP (2003) Differential metal selectivity and gene expression of two zinc transporters from rice. Plant Physiol **133:** 126–134

Rengel Z, Graham RD, Pedler JF (1994) Time-course biosynthesis of phenolics and lignin of wheat genotypes differing in manganese efficiency and resistance to take-all fungus. Ann Bot (Lond) **74:** 471–477

Stumm W, Morgan JJ (1981) Metal ions in aqueous solution: aspects of coordination chemistry. *In* JJ Morgan, ed, Aquatic Chemistry: An Introduction Emphasizing Chemical Equilibria in Natural Waters. John Wiley & Sons, New York, p 344

Williams LE, Pittman JK, Hall JL (2000) Emerging mechanisms for heavy metal transport in plants. Biochim Biophys Acta **1465:** 104–126

Wu Z, Liang F, Hong B, Young JC, Sussman MR, Harper JF, Sze H (2002) An endoplasmic reticulum-bound Ca^{2+}/Mn^{2+} pump, ECA1, supports plant growth and confers tolerance to Mn^{2+} stress. Plant Physiol **130:** 128–137